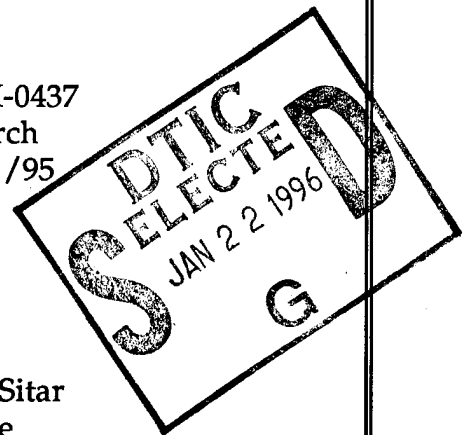# Quarterly Technical Report

Growth, Characterization and Device Development in Monocrystalline Diamond Films

R. F. Davis, R. J. Nemanich* and Z. Sitar
S. P. Bozeman and M. T. McClure
North Carolina State University
c/o Materials Science and Engineering Department
Box 7907
*Department of Physics
Raleigh, NC 27695

December, 1995

REPORT DOCUMENTATION PAGE

Form Approved
OMB No. 0704-0188

1. AGENCY USE ONLY *(Leave blank)*	2. REPORT DATE December, 1995	3. REPORT TYPE AND DATES COVERED Quarterly Technical 10/1/95–12/31/95

4. TITLE AND SUBTITLE

Growth, Characterization and Device Development in Monocrystalline Diamond Films

5. FUNDING NUMBERS

s400003srr14
1114SS
N00179
N66005
4B855

6. AUTHOR(S)

R. F. Davis, R. J. Nemanich, and Z. Sitar

7. PERFORMING ORGANIZATION NAME(S) AND ADDRESS(ES)

North Carolina State University
Hillsborough Street
Raleigh, NC 27695

8. PERFORMING ORGANIZATION REPORT NUMBER

N00014-93-I-0437

9. SPONSORING/MONITORING AGENCY NAMES(S) AND ADDRESS(ES)

Sponsoring: ONR, Code 312, 800 N. Quincy, Arlington, VA 22217-5660
Monitoring: Admin. Contracting Officer, ONR, Regional Office Atlanta
101 Marietta Tower, Suite 2805
101 Marietta Street
Atlanta, GA 30323-0008

10. SPONSORING/MONITORING AGENCY REPORT NUMBER

11. SUPPLEMENTARY NOTES

12a. DISTRIBUTION/AVAILABILITY STATEMENT

Approved for Public Release; Distribution Unlimited

12b. DISTRIBUTION CODE

13. ABSTRACT *(Maximum 200 words)*

X-ray photoelectron spectroscopy (XPS) has been conducted on a TiC(111) substrate to understand bias-enhanced nucleation (BEN) of CVD diamond. The data revealed two important results: i) the C:Ti ratio of the substrate decreases after an initial exposure to the biasing procedure, and ii) the C-C bonding signal is consistent with the formation of island-like deposition of an overlayer. The decrease in the C-Ti bonding signal suggests that BEN causes C vacancies to form. This procedure also appears to enhance the surface mobility of species on the surface allowing the rapid formation of carbon islands. Nuclear transmutation of B to Li is also being investigated for donor doping of diamond. Homoepitaxial ^{10}B enriched diamond films have been grown and characterized prior to irradiation using Hall measurements to determine resistivity, mobility and carrier concentration. The irradiation will be performed at Oak Ridge National Laboratory.

14. SUBJECT TERMS

diamond films, bias-enhanced nucleation (BEN), TiC(111) substrate, X-ray photoelectron spectroscopy (XPS), nuclear transmutation, boron, lithium, resistivity, mobility, carrier concentration, irradiation

15. NUMBER OF PAGES

15

16. PRICE CODE

17. SECURITY CLASSIFICATION OF REPORT	18. SECURITY CLASSIFICATION OF THIS PAGE	19. SECURITY CLASSIFICATION OF ABSTRACT	20. LIMITATION OF ABSTRACT
UNCLAS	UNCLAS	UNCLAS	SAR

Table of Contents

I. Introduction

Diamond as a semiconductor in high-frequency, high-power transistors has unique advantages and disadvantages. Two advantages of diamond over other semiconductors used for these devices are its high thermal conductivity and high electric-field breakdown. The high thermal conductivity allows for higher power dissipation over similar devices made in Si or GaAs, and the higher electric field breakdown makes possible the production of substantially higher power, higher frequency devices than can be made with other commonly-used semiconductors.

In general, the use of bulk crystals severely limits the potential semiconductor applications of diamond. Among several problems typical for this approach are the difficulty of doping the bulk crystals, device integration problems, high cost and low area of such substrates. In principal, these problems can be alleviated via the availability of chemically vapor deposited (CVD) diamond films. Recent studies have shown that CVD diamond films have thermally activated conductivity with activation energies similar to crystalline diamonds with comparable doping levels. Acceptor doping via the gas phase is also possible during activated CVD growth by the addition of diborane to the primary gas stream.

The recently developed activated CVD methods have made feasible the growth of polycrystalline diamond thin films on many non-diamond substrates and the growth of single crystal thin films on diamond substrates. More specifically, single crystal epitaxial films have been grown on the {100} faces of natural and high pressure/high temperature synthetic crystals. Crystallographic perfection of these homoepitaxial films is comparable to that of natural diamond crystals. However, routes to the achievement of rapid nucleation on foreign substrates and heteroepitaxy on one or more of these substrates has proven more difficult to achieve. This area of study has been a principal focus of the research of this contract.

At present, the feasibility of diamond electronics has been demonstrated with several simple experimental devices, while the development of a true diamond-based semiconductor materials technology has several barriers which a host of investigators are struggling to surmount. It is in this latter regime of investigation that the research described in this report has and continues to address.

In this reporting period, XPS was conducted on a TiC(111) substrate to understand bias-enhanced nucleation (BEN) of CVD diamond. A decrease in the C-Ti bonding signal suggests that BEN causes C vacancies to form. Enhanced surface mobility of species allows rapid formation of C islands. Homoepitaxial [10]B enriched diamond films have been grown and characterized prior to irradiation using Hall measurements to determine resistivity, mobility and carrier concentration. The following sections are self-contained in that they present an introduction, the experimental procedures, results and discussion, summary and indications of future research for the given research thrust.

II. Surface Analytical Study of the Bias-enhanced Nucleation of Diamond on Titanium Carbide(111)

A. Introduction

Epitaxial diamond films have been grown on both cBN and diamond [1-3]; however, these materials are expensive and large area substrates are not available. There has been past research to suggest that diamond heteroepitaxy may be achieved on other non-diamond or related substrates. The recent deposition on ß-SiC, Si, and Ni have shown the most dramatic results [4-10]. In the case of the work conducted on ß-SiC and Si, bias-enhanced nucleation (BEN) was used for the formation of these epitaxial diamond crystals [11]. The term highly oriented diamond (HOD) has been used to describe the partial alignment of individual grains. The individual particles may be epitaxial with respect to the substrate, however, tilting in both azimuthal and transverse directions results in the formation of low-angle grain boundaries [12]. The origin of this misalignment is believed to be a result of an approximately 22% mismatch at the diamond/SiC interface [9]. Recently, the use of the BEN procedure on TiC(111) has resulted in the deposition of oriented diamond particles [13].

Despite the number of substrates that have resulted in oriented diamond deposition, understanding the nucleation mechanism remains elusive. To gain further understanding, a surface analytical (XPS and LEED) investigation of TiC(111) after sequential exposures to the BEN procedure was undertaken. The structural and chemical information these two techniques can provide are exceptionally useful to describe surface changes during the bias-enhanced nucleation process.

B. Experimental Procedure

Upon receiving the samples from Advanced Technology Materials, Inc., the samples were polished using progressively finer media. The polishing scheme started with 600 grit SiC, then 30µm diamond and progressing through 6µm, 1µm, and 0.1µm diamond and finishing with one hour of 0.05µm Al_2O_3 powder to remove any residual diamond detritus that may have been embedded in the TiC surface. Then the samples were cleaned using acetone, methanol, and isopropanol. After polishing and characterization of the substrate surface, the sample was loaded into the deposition chamber and subjected to a H_2 plasma cleaning to remove any advantitious hydrocarbon adsorbates. Table I summarizes the system parameters that resulted in the deposition of oriented diamond particles [13]. For the analytical series, the same BEN conditions were used for 5 minute intervals and the sample was transferred *in vacuo* to the surface analytical system.

**Table I. Summary of MPCVD System Parameters
Used to Deposit Oriented Diamond Particles.**

System Parameter	H$_2$ Plasma Cleaning	BEN	Growth
Power (W)	600	600	600
Pressure (Torr)	25	15	40
CH4:H2 ratio	...	5%	0.2%
Bias current (mA)	...	120	...
Bias current (Vdc)	...	225±10	...
Temperature (°C)	660±20	785±20	900
Duration	30 min	10-15 min	8 h

C. Results of Surface Analytical Examination

Results of LEED Analysis. After the H$_2$ plasma cleaning, the sample was transferred into the surface analytical chamber and a LEED pattern was observed. The pattern was consistent with a {111}-(1×1) structure expected for the TiC(111) face. A LEED pattern was obtained only after the H$_2$ plasma cleaning stage and not at any other time of experiment. The formation of islands or loss of symmetry on the surface by amorphization or polycrystallization would have resulted in the loss of a LEED pattern.

Results of XPS Analysis. Low energy electron diffraction was used to determine the structure of the surface but could not provide information about the chemical nature of the surface. To gain chemical identification and bonding information about the species on the surface x-ray photoelectron spectroscopy (XPS) was also performed after each period of the BEN series. XPS provided elemental identification of surface and sub-surface species and, by detecting any shift from the elemental peak position, XPS also supplied information about the bonding nature of the elements detected. Examination of the peak intensities as a function of time provided information about structure of an overlayer that is being deposited. Detailed explanation of each aspect of XPS analysis is provided in the relevant sections.

Peak Identification. Initially a low resolution scan, termed a "survey scan," of the surface was performed for elemental identification. Examination of this spectrum indicated that oxygen, titanium, and carbon were present on the surface. To gain bonding information a higher resolution scan over the particular peak energies were performed. The XPS spectra for each energy region and step in the temporal series are shown Fig. 1(a-c). The peak centers and area intensities were determined by fitting the spectra to Voigt peaks, which are a combination of Gaussian and Lorentzian peaks, using the IGOR Pro software from Wavemetrics, Inc. In all stages some residual oxygen was detected, but the photoelectron peak was broad indicating that the oxygen was only weakly bound to the surface and may have adsorbed during transfer between chambers. Importantly, peaks that would indicate oxygen bonding with titanium were

3

absent. The high binding energy features in some of the C1s spectra were due to some of the residual oxygen binding to carbon species to form a C-O complex. The feature appeared again only in the spectrum taken after 25 minutes of biasing and may have formed while the substrate cooled after the plasma was extinguished. The other features in the C1s spectra were characteristic of C-C bonding (285 eV) and C-Ti (282 eV) bonding. In the Ti2p region only those features indicative of Ti-C (455 eV) bonding were present [14, 15].
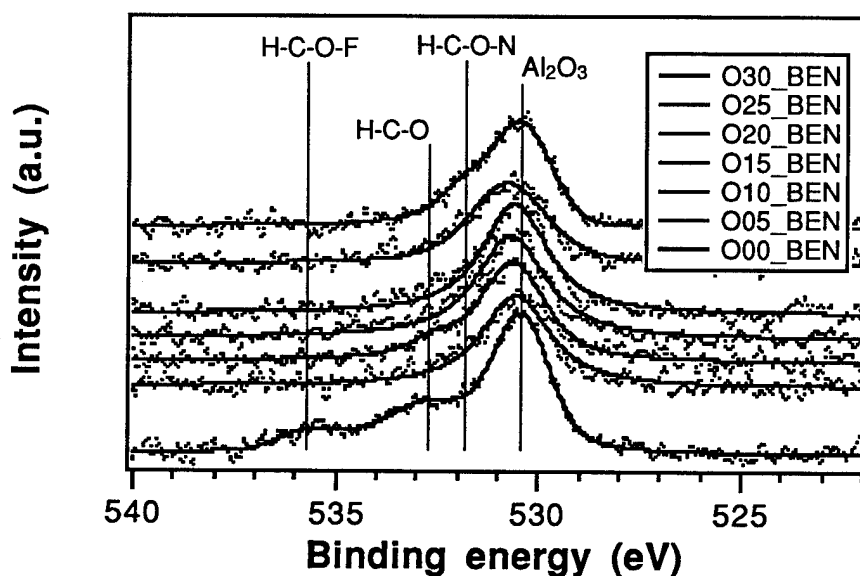

Figure 1(a).   XPS spectra for the O1s photoelectron energy. Energy positions for relevant species are shown.
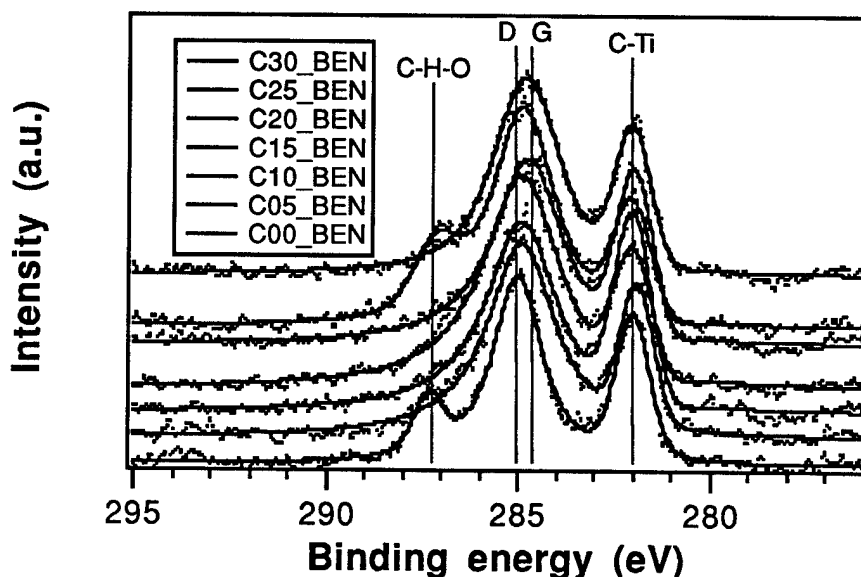

Figure 1(b).   XPS spectra for the C1s photoelectron energy. Energy positions for relevant species are shown.
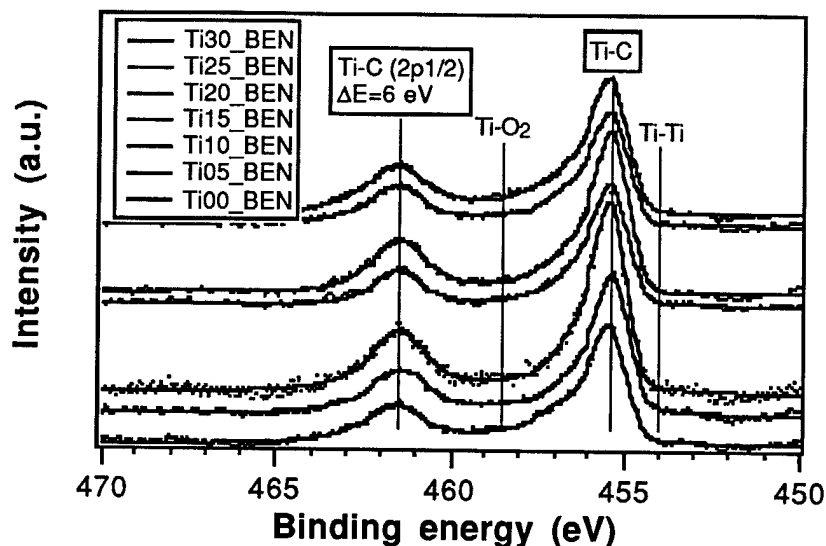
Figure 1(c).   XPS spectra for the Ti2p photoelectron energy. Energy positions for relevant species are shown.

Compositional Analysis. Compositional and overlayer thickness calculations were made given the peak area intensities determined by curve fitting the XPS spectra. By comparing the area intensity of the C-Ti (282 eV) peak to the Ti-C (455.5 eV) peak the composition of the surface was determined (Fig. 2). Equation 1 was used to calculate the C:Ti ratio for each time step examined and the results are shown in Fig. 3. After 5 minutes of the BEN procedure, the C:Ti ratio decreased dramatically and leveled off after 15 minutes of biasing [14].

$$n_C/n_{Ti} = (I_C/I_{Ti})\,\sigma_{Ti}/\sigma_C \tag{1}$$

where n_{Ti} and n_C are the concentrations of Ti and C, respectively,

I_C and I_{Ti} are the peak areas of the C1s and Ti2p peaks, respectively, and

σ_{Ti} and σ_C are the photoionization cross sections of Ti and C, respectively.

The decay of the C:Ti ratio with BEN duration suggested that the composition of the substrate in the near surface region became carbon deficient. Because the peak intensity of the Ti-C peak (455 eV) did not increase with time, the data did not suggest that the near surface region became Ti abundant rather the C-Ti peak (282 eV) decrease with time suggested carbon deficiency. One explanation for the decrease in the C:Ti ratio was the formation of carbon vacancies by ion bombardment as a result of the applied negative substrate potential. The displaced carbon atoms could have been knocked into interstitial positions where they remained or migrated to the surface. This data provided clues to the BEN mechanism but no clear answers.
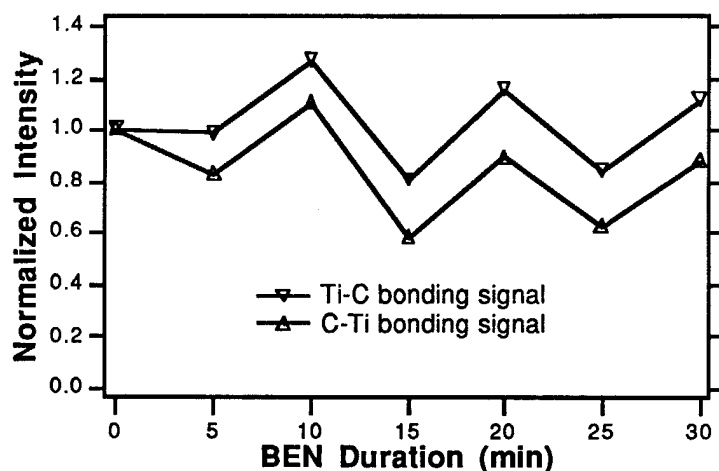
5

Figure 2.   The normalized photoelectron intensity for the C-Ti and Ti-C bonding as a function of BEN duration.
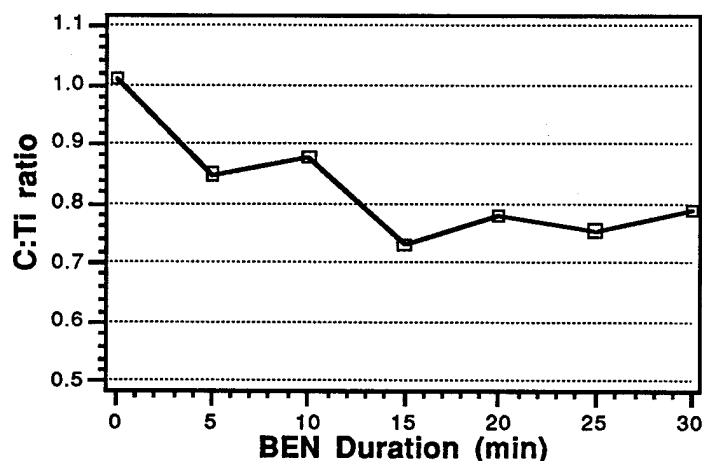

Figure 3.   C:Ti ratio as a function of BEN duration. The ratio was calculated using Eq. 1.

Overlayer Information. The decay in intensity of the photoelectrons can be used to determine the growth of the overlayer. The attenuation is due to the exponential probability of electrons escaping the surface without suffering inelastic collisions with atoms in the overlayer. The shape of the attenuation curve supplies information for determining the growth mode. If the growth mode is "layer-by-layer" then the intensity of the substrate photoelectron peak can be written as:

$$I_S/I_{So} = (1-x)\exp[-nl/\lambda] + x\exp[-(n+1)l/\lambda]$$
(2)

where I_S and I_{So} are the peak intensities for the substrate with an overlayer present and for the clean substrate, respectively,

l is the monolayer thickness,

6

λ is the inelastic mean free path of the photoelectron,

(1-x) is the fraction of the surface covered with n layers, and

x is the fraction of the surface covered with (n+1) layers.

If the growth mode is "islanding," the attenuation curve is not a simple exponential because some of substrate will always be exposed to eject electrons and the substrate signal will persist for significant amounts of material deposited. To correctly interpret an electron yield curve in this case would require an accurate knowledge of the surface coverage of the islands and knowledge of the mean free path of the electrons. An intermediate case occurs when islands form after a few initial layers have deposited in a "layer-by-layer" fashion. This growth mode is termed "layer-plus-islanding." In this case the attenuation curve follows an exponential decay as long as the deposition is "layer-by-layer," but afterwards the signal from the substrate persists. The equation below illustrates this type of attenuation for the case where islands two monolayers high cover 50% of the surface after the initial monolayer has deposited uniformly.

$$I_S/I_{So} = (1-x)\exp[-l/\lambda] + x\exp[-3l/\lambda], \qquad 0 \leq x \leq 0.5, \qquad (3)$$

where all variables have the same meaning as in Eq. 2.

The attenuation curves for all three growth modes are illustrated in Figure 4(a). Curves for the intensity increase overlayer can also be modeled and they have similar shapes according to the growth mode but increase with the form of $1-e^x$ (Fig. 4(b)) [14].

The non-zero value of the C-C signal after the H_2 plasma cleaning and the apparent saturation of the signal from BEN times 15 - 30 minutes allowed two different analyses. First, the C-C signal intensity has been normalized to show the increase in the signal after the H_2 plasma cleaning. The shape of this curve was indicative of a "islanding" deposition mode. Second, the C-C intensity was normalized assuming the signal from 15 to 30 minutes was a maximum signal and has a relative value of 1. Using this method, the thickness of the carbon layer after the H_2 plasma cleaning was calculated according to Eq. 2, assuming the remaining C-C signal comes from an equivalent uniform thickness. Combining these two analysis methods, the C-C signal indicated that the carbon layer was equivalent to one monolayer of TiC (i.e., the TiC(111) plane was carbon terminated) and the deposited carbon islands covered 55% of the substrate surface.

D. Summary

The proof-of-concept deposition on the TiC(111) substrate proved successful with the observation of oriented diamond particles and a characteristic Raman spectra. A surface analysis series was performed after 5 minute periods of the biasing procedure. Analysis of the
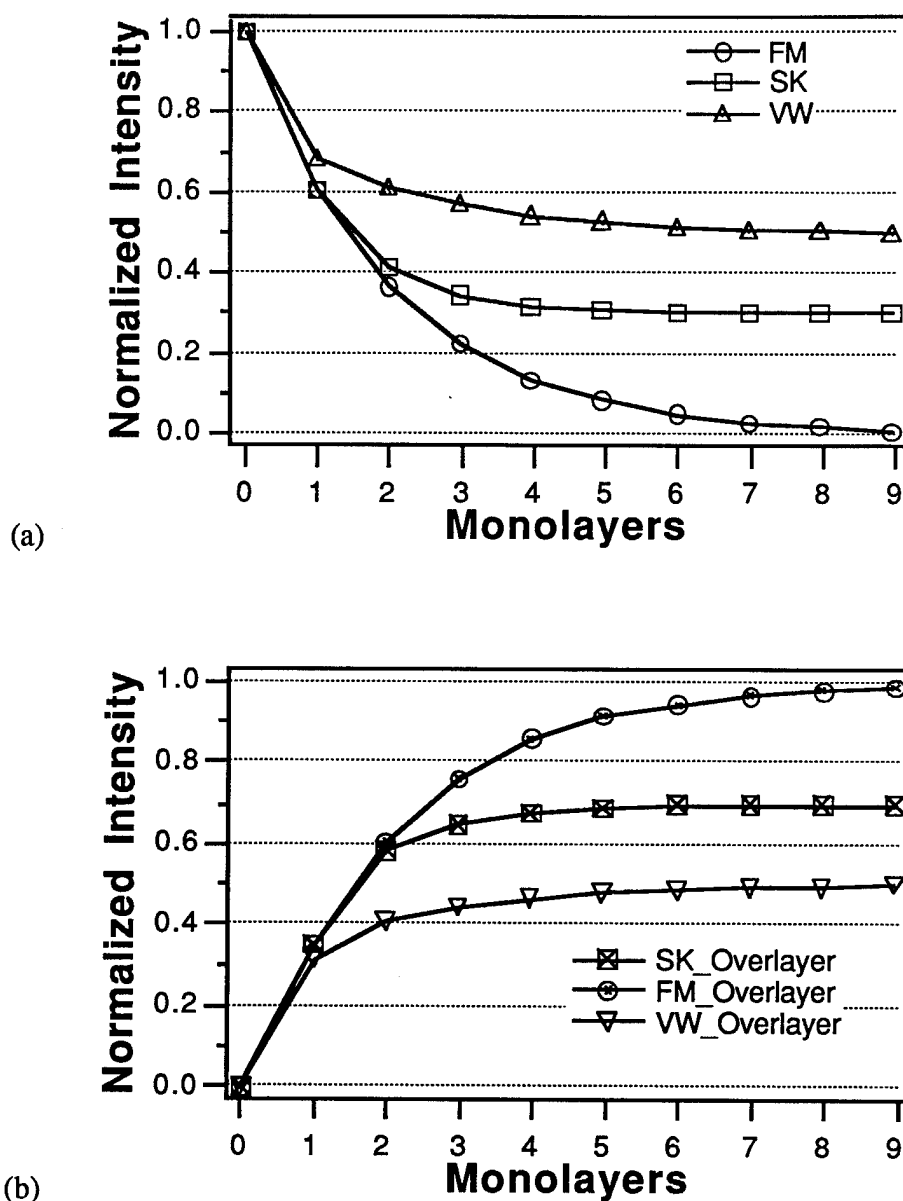
(a)

(b)

Figure 4.   Attenuation curves for (a) substrate and (b) overlayer photoelectrons as a function of average coverage of an overlayer. In these examples the mean free path is taken as 2 monolayers and the islands cover 50% of the surface.

C1s photoelectron spectra revealed three important results: i) the substrate (TiC(111) plane) was carbon terminated, ii) the BEN process caused carbon vacancies on TiC as noted from the decay of C-Ti photoelectron signal, and iii) the resultant carbon was deposited in a "island-like" growth mode. These results suggested the BEN process formed vacancies similar to an ion implantation technique and may have increased the surface mobility of C atoms so they can migrate to form islands.
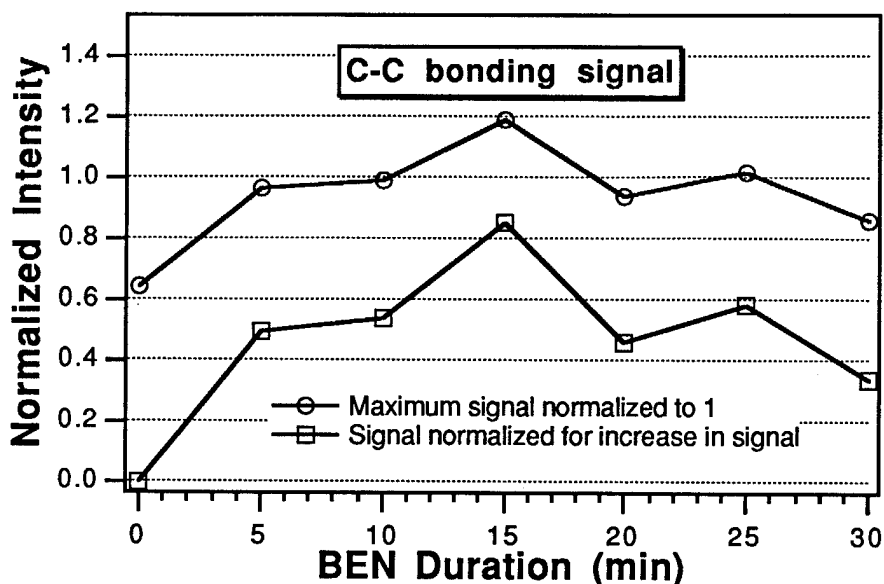
Figure 5.   The normalized photoelectron intensity for C-C bonding as a function of BEN duration.

E. References

1. H. Meada, S. Masuda, K. Kusakabe and S. Morooka, Dia. Rel. Mat. **3**, 398 (1994).
2. S. Koizumi, T. Murakami, T. Inuzuka and K. Suzuki, Applied Physical Letters **57** (6), 563 (1990).
3. M. Kamo, H. Yurimoto and Y. Sato, "Epitaxial growth of diamond on diamond substrate by plasma assisted CVD" in *Proceedings of Proceedings of the Fourth International Conference on Solid Films and Surfaces (ICSFS-4),* Aug 23-27 1987, Hamamatsu, Jpn., edited by p. 553-560.
4. B. R. Stoner, G. H. Ma, S. D. Wolter, W. Zhu, Y.-C. Wang, R. F. Davis and J. T. Glass, Dia. Rel. Mat. **2**, 142 (1993).
5. B. R. Stoner, "Bias Enhanced Nucleation and Heteroepitaxial Growth of Diamond by Microwave Plasma Chemical Vapor Deposition," Doctor of Philosophy thesis, North Carolina State University, 1992.
6. P. C. Yang, W. Zhu and J. T. Glass, Journal of Materials Research **8** (8), 1773 (1993).
7. S. D. Wolter, B. R. Stoner, J. T. Glass, P. J. Ellis, D. S. Buhaenko, C. E. Jenkins and P. Southworth, Appl. Phys. Lett. **62** (11), 1215 (1993).
8. Y. Sato, I. Yashima, H. Fujita, T. Ando and M. Kamo, "Epitaxial Growth of Diamond from the Gas Phase" in *Proceedings of New Diamond Science and Technology,* Washington, D.C., September 23-27, 1990, edited by R. Messier, J. T. Glass, J. E. Bulter and R. Roy, (Materials Research Society, Pittsburgh, PA, 1991) p. 371.
9. X. Jiang, C.-P. Klages, R. Zachai, M. Hartweg and H.-J. Füsser, Appl. Phys. Lett. **62** (26), 3438 (1993).
10. C. Wild, R. Kohl, N. Herres, W. Müller-Sebert and P. Koidl, Dia. Rel. Mat. **3**, 373 (1994).
11. B. R. Stoner and J. T. Glass, Appl. Phys. Lett. **60** (6), 698 (1992).
12. W. Zhu, X. H. Wang, B. R. Stoner, G. H. M. Ma, H. S. Kong, M. W. H. Braun and J. T. Glass, Phys. Rev. B **47** (11), 6529 (1993).
13. S. D. Wolter, M. T. McClure, J. T. Glass and B. R. Stoner, Appl. Phys. Lett. **66** (21), 2810 (1995).
14. L. C. Feldman and J. W. Mayer, *Fundamentals of Surface and Thin Film Analysis,* (Elsevier, New York, 1986), p. 352.

III. Donor Doping of Diamond Using Nuclear Transmutation

A. Introduction

Nuclear transmutation has been proposed for donor doping of diamond [1]. The goal of this process is to convert boron incorporated during growth to interstitial lithium through the reaction $^{10}B(n,\alpha)^7Li$. Calculations indicate that interstitial Li in diamond produces a shallow acceptor state [2]. This doping mechanism is of interest in diamond because of difficulties encountered in attempts to incorporate Li by more conventional means such as diffusion or incorporation during CVD. A similar transmutation process has been used for low and uniform doping of Si with P for high power applications through the conversion $^{30}Si(n,\gamma)^{31}Si$ which then decays to ^{31}P. Some important differences between the two processes are the nature of the atom to be converted and the effect of radiation damage on the lattice. First, for the case of boron in diamond, one is converting a acceptor dopant to a donor dopant. As a result, a large majority, probably greater than 90%, of the boron must be converted to avoid compensation, requiring a large neutron dose. Secondly, the diamond lattice can be irreversibly converted to graphite if the radiation damage is too great.

Previous work in this area has included neutron irradiation of ^{10}B doped polycrystalline films and annealing studies of the resulting damage. These studies indicated that damage from doses as large as 2.6×10^{20} n/cm^{-2} could be recovered by annealing [3]. However, electrical measurements have not been reported.

There are several technical and scientific challenges that must be overcome in evaluating the transmutation of boron in diamond. A suitable source of isotopically pure ^{10}B must be identified. A high neutron flux must be available, as a dose of 5×10^{20} n/cm^2 is estimated to be necessary to convert a large fraction of the ^{10}B and avoid compensation. Evaluation of electrical measurements made after irradiation must be done with care, as irradiation damage can lead to defect conduction. In addition, grain boundaries can alter both conduction and diffusion processes if polycrystalline films are used [4]. Furthermore, the possibility of lithium diffusion through the lattice after conversion must be considered.

In response to these challenges, our approach has been to investigate transmutation in well characterized homoepitaxial films grown by established techniques. Growth and electrical measurements have been performed at Kobe Steel USA by researchers with extensive experience in electrical measurements on homoepitaxial and polycrystalline diamond film. Our isotopically pure boron source is diborane, one of the most common doping sources of boron for CVD diamond growth. The carrier concentration and mobility have been measured as a function of temperature prior to irradiation. In addition, our experiments include control samples with no boron and with the natural abundance of boron to separate the effects of irradiation damage from the effects of Li production. We are also in contact with a group at Oak

10

Ridge National Laboratory which can provide a neutron flux of 2×10^{15} n/cm^{2}s which can produce the desired dose in 3 days of continuous irradiation.

Table I. Samples and target boron content. All films are grown
on (100) oriented type 2a natural diamond substrates.
The natural isotopic abundance of boron is 19% ^{10}B and 81% ^{11}B.

Sample	Boron Content (Target value, cm^{-3})	Isotopic Composition
1	10^{18}	natural abundance
2	10^{20}	natural abundance
3	10^{18}	^{10}B enriched
4	10^{20}	^{10}B enriched
5	10^{20}	^{10}B enriched

B. Experimental Procedure

Homoepitaxial boron doped films have been grown using microwave CVD with diborane as to dopant source. Growth conditions were similar to previously reported work by researchers at Kobe Steel USA [5]. Table I shows the target boron concentrations for each of the five films. All films are grown on (100) oriented type 2a natural diamond substrates and range from 3 to 8 microns in thickness. The films were grown over a 3×3mm^2 area on the 4×4mm^2 substrates to isolate the films from the edges of the wafers. The edges of natural diamond wafers have a higher conductivity which has lead to anomalous results in the past. This selected area deposition also facilitates measurement of the film thickness. Films with the natural abundance of the two boron isotopes are included to aid in separating the effects of Li production from the effects of damage. The natural isotopic abundance of boron is 19% ^{10}B and 81% ^{11}B, so the maximum possible conversion of the natural abundance samples (#1 and #2) is 19%. Samples 4 and 5 have the same boron content to provide a duplicate experiment. In addition, measurements can be made of the back surfaces of the diamond wafers to analyze the effects of neutron irradiation on diamond which is free of boron.

Metal contacts consisting of Ti and Au were applied. The carrier concentration and mobility were measured at several temperatures from 300 to 600 K using the Hall effect in a van der Pauw geometry. Descriptions of the metallization process and Hall measurements can be found in publications by researchers at Kobe Steel [5].

C. Results and Discussion

The measured room temperature values of resistivity, mobility, and carrier concentration for the five films are given in Table II. These quantities are plotted as a function of temperature

11

in Fig. 1 (resistivity), Fig. 2 (mobility), and Fig. 3 (carrier concentration). The two samples with lower boron concentrations yield similar results in the electrical measurements, as do the more heavily doped samples. Mobility values are lower for the more highly doped samples, as would be expected. Samples 4 and 5 with the same target boron concentration vary in carrier concentration be nearly a factor of 10. This variation could be caused by different doping levels or by different percentage activation. The true boron concentration will be measured via SIMS after the irradiation experiments are completed. SIMS measurements have been deferred to avoid possible damage to the samples.

Table II. Room Temperature Values of Resistivity, Mobility, and Carrier Concentration for Homoepitaxial Boron-doped Films Which Will be Irradiated.

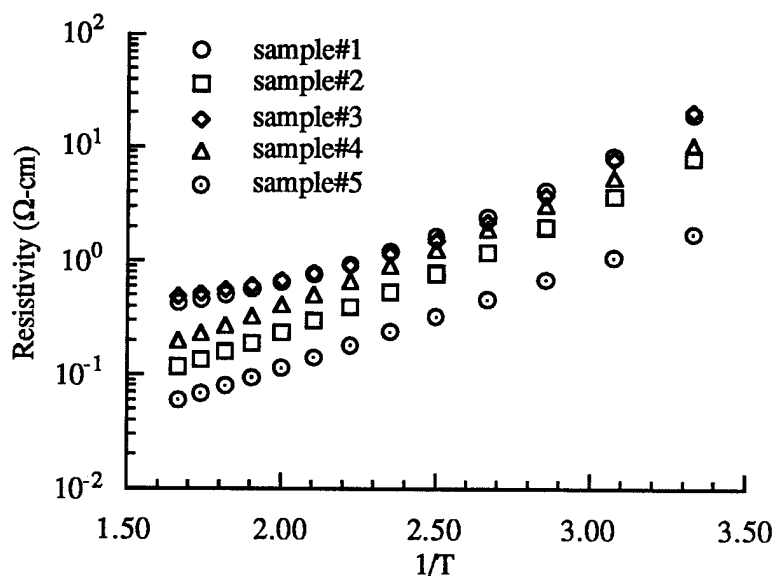| Sample	Boron content (Target, cm^{-3})	Thickness (μm)	Resistivity (Ω-cm)	Mobility (cm^2/Vs)	Carrier Concentration (cm^{-3})
1	10^{18}	6.2	19	933	3.49×10^{14}
2	10^{20}	5	8	53	1.50×10^{16}
3	10^{18}	8	20	1160	2.70×10^{14}
4	10^{20}	5.5	10	62	9.91×10^{15}
5	10^{20}	3.3	2	32	1.13×10^{17}

Figure 1.   Resistivity as a function of 1/T for the five homoepitaxial films which will be irradiated.
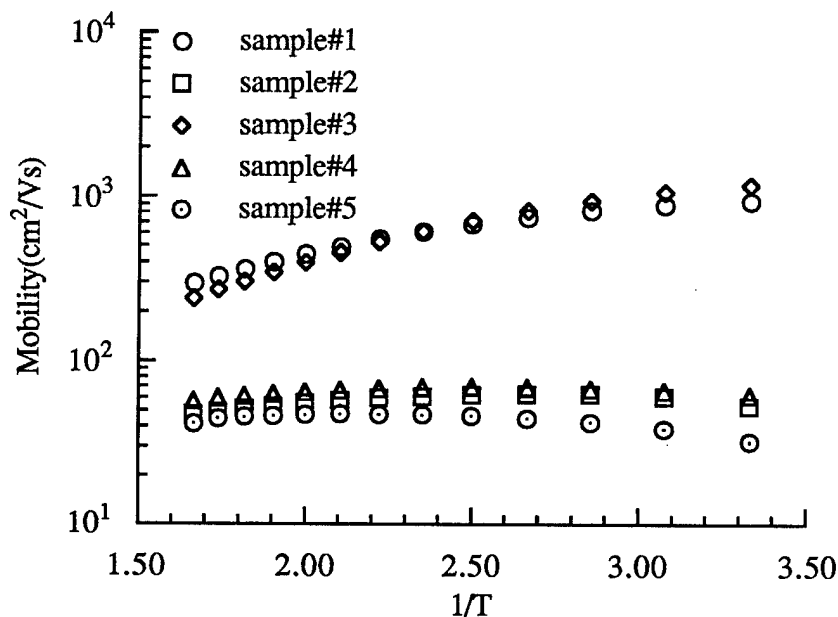
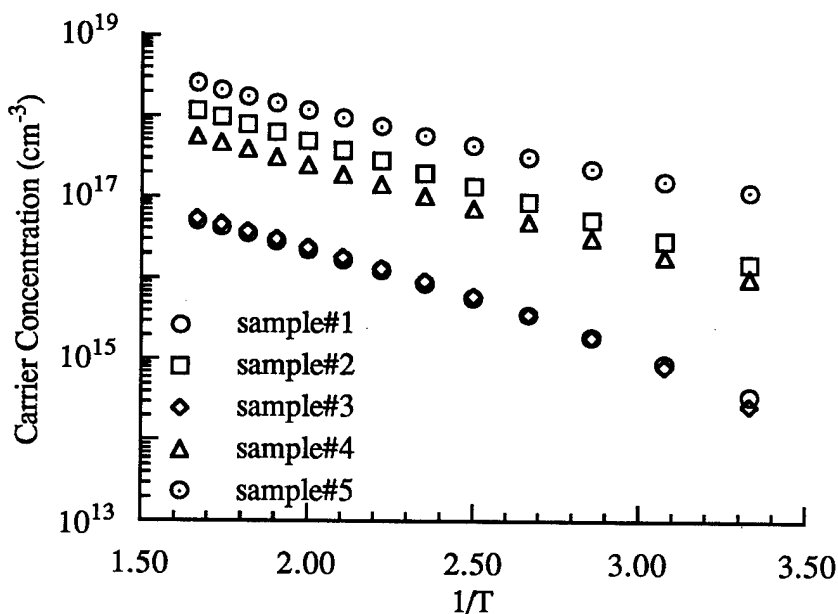Figure 2.   Hole mobility as a function of 1/T for the five homoepitaxial films which will be irradiated.

Figure 3.   Carrier concentration (p-type) as a function of 1/T for the five homoepitaxial films which will be irradiated.

D. Conclusions

In summary, nuclear transmutation is being investigated as a means for donor doping of diamond. To date samples have been prepared for irradiation and baseline electrical measurements have been performed.

13

E. Future Research Plans and Goals

The next steps in the project are (1) completion of pre-irradiation characterization, (2) neutron irradiation, (3) characterization and annealing studies post irradiation. The complexity of the post irradiation studies will be determined by the amount of damage produced in the irradiation process. Post irradiation studies will begin with optical assessment of the damage via Raman and Photoluminescence spectroscopy. Electrical characterization via I-V measurements and Hall effects measurements will then be performed. If the carrier type is changed by the irradiation process, different contact materials may be necessary. Following the electrical measurements SIMS can be used to measure the percentage of boron converted to lithium. Finally, if the electrical measurements are promising, RBS-channeling may be used to determine the lattice location of the lithium.

F. References

1. B. Spitsyn, G. Popovici and M. A. Prelas, *Second International Conference on the Applications of Diamond Films and Related Materials*, edited by M. Yoshikawa, M. Murakawa, Y. Tzeng and W. A. Yarbrough, Tokyo, Japan, 1993, 57-64.
2. S. A. Kajihara, A. Antonelli, J. Bernholc and R. Car, Physical Review Letters **66**, 2010 (1991).
3. S. A. Khasawinah, G. Popovici and H. White, Journal of Materials Research **10**, 2523 (1995).
4. J. Y. W. Seto, Journal of Applied Physics **46**, 5247 (1975).
5. D. M. Malta, J. A. v. Windheim, H. A. Wynands and B. A. Fox, Journal of Applied Physics **77**, 1536 (1995).

IV. Distribution List

Mr. Max Yoder   3
Office of Naval Research
Electronics Division, Code: 312
Ballston Tower One
800 N. Quincy Street
Arlington, VA 22217-5660

Administrative Contracting Officer   1
Office of Naval Research
Regional Office Atlanta
101 Marietta Tower, Suite 2805
101 Marietta Street
Atlanta, GA 30323-0008

Director, Naval Research Laboratory   1
ATTN: Code 2627
Washington, DC 20375

Defense Technical Information Center   2
Bldg. 5, Cameron Station
Alexandria, VA 22314